

Energy Efficiency and Blocking Reduction for Tidal Traffic via Stateful Grooming in IP-Over-Optical Networks

Zhizhen Zhong, Nan Hua, Massimo Tornatore, Yao Li, Haijiao Liu, Chen Ma, Yanhe Li, Xiaoping Zheng, and Biswanath Mukherjee

Abstract—The growing popularity of high-speed mobile communications, cloud computing, and the Internet of Things (IoT) has reinforced the tidal traffic phenomenon, which induces spatio-temporal disequilibrium in the network traffic load. The main reason for tidal traffic is the large-scale population migration between business areas during the day and residential areas during the night. Traffic grooming provides an effective solution to aggregate multiple fine-grained IP traffic flows into the optical transport layer by flexibly provisioning lightpaths over the physical topology. In this paper, we introduce a comprehensive study on energy efficiency and network performance enhancement in the presence of tidal traffic. We propose and leverage the concept of *stateful grooming* to apply differentiated provisioning policies based on the state of network nodes. We formulate and solve the node-state-decision optimization problem, which can decide the specific state of network nodes when a certain traffic profile is given, considering the trade-off between energy efficiency and blocking performance with a multi-objective integer linear program (MOILP). Then, we propose an online traffic-aware intelligent differentiated allocation of lightpaths (TIDAL) algorithm, based on stateful grooming and the MOILP, to accommodate the dynamic tidal traffic. Our illustrative numerical results show that the proposed method can achieve a significant performance improvement in an energy-efficient way.

Index Terms—Energy efficiency; Grooming; IP-over-optical network; Network optimization; Spatio-temporal disequilibrium; Tidal traffic.

Manuscript received September 2, 2015; revised January 8, 2016; accepted January 12, 2016; published March 1, 2016 (Doc. ID 248178).

Zhizhen Zhong is with the Tsinghua National Laboratory for Information Science and Technology, Department of Electronic Engineering, Tsinghua University, Beijing 100084, China. He is also a visiting Ph.D. student at the Networks Lab at the University of California, Davis, California 95616, USA.

Nan Hua, Yao Li, Haijiao Liu, Yanhe Li, and Xiaoping Zheng (e-mail: xpzheng@mail.tsinghua.edu.cn) are with the Tsinghua National Laboratory for Information Science and Technology, Department of Electronic Engineering, Tsinghua University, Beijing 100084, China.

Massimo Tornatore is with the Department of Electronics, Information and Bioengineering, Politecnico di Milano 20133, Italy. He is also with the Networks Lab at the University of California, Davis, California 95616, USA.

Chen Ma is with the State Key Laboratory of Information Photonics and Optical Communications, Beijing University of Posts and Telecommunications, Beijing 100876, China. He is also a visiting Ph.D. student at the Networks Lab at the University of California, Davis, California 95616, USA.

Biswanath Mukherjee is with the Networks Lab at the University of California, Davis, California 95616, USA.

<http://dx.doi.org/10.1364/JOCN.8.000175>

I. INTRODUCTION

Tidal traffic, characterized by periodic dynamics of traffic load in joint temporal and spatial domains, is an emerging traffic pattern caused by the popularity of high-speed mobile Internet as well as the increase of data service driven by cloud computing and the Internet of Things (IoT). This new scenario poses a serious problem to the network operation and management [1], as the network traffic is no longer distributed uniformly: there can be a huge gap between the traffic peak and traffic valley at any moment, while the peak and valley may also shift over time. For example, in fast-developing countries like China, India, and Brazil, the urbanization process is resulting in megalopolises with over 10 million people [2], while in developed countries, the metropolitan agglomerations like the San Francisco Bay Area and the Paris metropolitan area also maintain a large population within a certain area. In such locations, the districts are divided into several functional areas, like business areas and residential areas, and the huge population migration between the areas for daily commutes drives the network traffic to also fluctuate in the same daily pattern. The business areas of the city will experience much more traffic than the residential areas during the daytime, while the traffic pattern will be the opposite at night as people move from their workplaces to their residences after work. Moreover, the Cisco Visual Networking Index white paper indicates that the global IP traffic will increase threefold over the next five years [3], while the global mobile Internet traffic will increase nearly tenfold [4]. Thus, the faster growth of mobile traffic as well as the urbanization with metropolitan agglomerations will deepen the influence of tidal traffic, making it an important issue for network operators.

Generally, tidal traffic degrades the network performance for two reasons. In peak traffic areas, the network blocking may increase due to the sharp increase of traffic, while network nodes may stay idle with little traffic in valley traffic areas, wasting a large amount of energy. However, both service performance and the energy efficiency [5] are important properties for communication networks; thus, there is a growing need to provide solutions to the problem of tidal traffic.

Tidal traffic was first studied in wireless networks in a small area consisting of several neighboring base stations [6]. Later, with the growth of communications demands and networking technologies, the affected scope in the spatial and temporal domains as well as the degree of severity of tidal traffic are increasing, and the tidal traffic further affects the optical access networks, and even optical metro or core networks.

To design an energy-efficient network, Ahmed *et al.* [7] proposed an efficient resource-management technique for wireless optical access networks that reduces the power consumption by introducing sleep modes for the optical line terminals and optical network units, based on the service class and traffic load; however, its limitation is that it uses the aggregated traffic of the whole network, neglecting the spatial disequilibrium of the traffic distribution. Wang *et al.* [8] put forward an energy-efficient investigation on tidal traffic, considering both the temporal and spatial domains in optical access networks using wavelength sharing in time- and wavelength-division-multiplexed passive optical networks (TWDM-PON), but its limitation is that it focuses on the access network, and only achieves energy savings by turning off the idle access equipment and setting them to sleep mode selectively, without considering the increased availability to accommodate more traffic under peak hours.

The main limitations of these previous studies are that their methods are based on access networks, and they were trying to consolidate the traffic into fewer resources in order to power off the rest of the infrastructure to achieve energy efficiency. However, if we consider optical metro or core networks, previous approaches such as turning off idle equipment may not be useful, as the difference between access network equipment and core or metro networks is that we cannot simply turn off the entire optical node equipment, even during idle periods. This is because the core or metro network nodes are the basis of the communication system, so they must be operational at all times. Therefore, the energy-aware design for multi-layer networks [9] is a possible solution to tidal traffic in core or metro networks. Similar to the research in access networks, most previous works focus on the uneven distribution of traffic in temporal domains [10,11], and neglects the disequilibrium of tidal traffic in spatial domains. Rizzelli *et al.* [12] presented a power-aware multi-layer design for daily traffic variation in core IP-over-optical networks; however, its limitation is that it did not consider the spatial disequilibrium of tidal traffic and focused only on energy savings without improving the service quality for traffic peaks. Coiro *et al.* [13] reduced the power consumption in wavelength-routed networks by selectively switching off optical links, and Zhang *et al.* [14] presented an energy-optimized design for an IP-over-optical network. Lange and Gladisch [15] studied the energy-efficiency limits of these adaptive networks. Therefore, we need new approaches to achieve energy efficiency as well as blocking reduction.

In [16], we proposed a brief solution to tidal traffic in a dynamic scenario without considering energy efficiency.

Here, in this extended version of the study, we present a comprehensive investigation on tidal traffic in IP-over-optical networks. We summarize the contributions of this work as follows: (1) to the best of our knowledge, this is the first investigation on solving the tidal-traffic problem with disequilibrium in temporal and spatial domains in IP-over-optical metro or core networks; (2) we introduce and leverage the concept of *stateful grooming* to analyze the operational state of network nodes according to the traffic load, thus applying differentiated grooming policies to accommodate the tidal traffic to the maximum extent possible; (3) we formulate the node-state-decision optimization problem into a multi-objective integer linear program (MOILP) problem by considering the trade-off between energy efficiency and blocking reduction, and solve the problem via the Pareto front principle, by adopting different quality of service (QoS) criteria, so we can achieve energy savings without any blocking loss, or even larger energy savings with an acceptable blocking compromise; and (4) an effective online algorithm on the basis of the stateful grooming and MOILP results is proposed to solve the dynamic tidal traffic problem.

The rest of this paper is organized as follows. Section II proposes the concept of stateful grooming as well as the node-state-decision model. In Section III, we formulate the model by considering the trade-off between energy efficiency and blocking performance in a static scenario. We present a dynamic traffic-aware intelligent differentiated allocation of lightpath (TIDAL) scheme to handle tidal traffic effectively in Section IV on the basis of static planning. In Section V, we design the workflow procedures of the dynamic scheme with a software-defined architecture. Section VI shows the numerical evaluation, and Section VII concludes this study.

II. STATEFUL GROOMING

Traffic grooming in multi-layer networks such as IP-over-optical networks [17] enables fine-grained traffic to be aggregated into high-bandwidth lightpaths provisioned on physical optical networks. It has been an active research area in recent years. Zhu *et al.* [18] proposed a novel generic graph model for traffic grooming in heterogeneous wavelength-division-multiplexed (WDM) mesh networks. In [19], the authors give a systematic introduction and study on traffic-grooming problems in various circumstances. Zhu and Mukherjee [20] reviewed the work on traffic grooming in WDM networks. For multi-layer IP/optical networks, the dynamic traffic-grooming problem is solved in [21]. In [22,23], an iterative algorithm for efficient traffic grooming in a multi-layer Internet protocol/multi-protocol label switching (IP/MPLS) over a meshed optical transport network scenario is presented, which allows us to plan a cost-effective IP/MPLS logical topology over an optical topology to deal with the offered traffic pattern.

Today, the traffic distribution patterns have greatly changed, as stated above, and new problems like tidal traffic need to be tackled for traffic grooming.

A. Grooming States

Inspired by the simple principle that a *specific condition needs specific analysis*, we define different grooming states on the basis of previous research and apply them in different traffic situations. In particular, the main issue in busy areas (heavy traffic load in the static case, or high traffic arrival rate in the dynamic case) is to make the most use of the wavelength resources in this area to accommodate more traffic and decrease the resource occupation of other transients, especially optical bypass traffic. This state is defined as the *tide-peak* state.

Meanwhile, the main issue in idle areas (light traffic load in the static case, or low traffic arrival rate in the dynamic case) is to guarantee the access capacity while providing more availability for other traffic to transit and save energy. This state is defined as the *tide-valley* state, which is also the default state of the node. So, we propose to adopt optical bypass in idle nodes to provide spare resources for bypassing lightpaths to support flexible logical links for energy efficiency, while we forbid optical bypass in busy nodes to ensure that all the physical resources are exploited to accommodate the peak traffic requests to reduce blocking. Hence, the node can shift between these two states according to traffic fluctuations.

B. Node-State-Decision Model

Figure 1 shows how a node operates if it is selected as the tide-peak node. We consider multi-layer IP-over-optical networks consisting of the IP/MPLS layer and the optical layer. The optical layer can provide resources for virtual links in the upper IP/MPLS layer. Each optical cross-connect (OXC) and IP/MPLS node pair denotes one actual IP/optical integrated node. To explain the model, we assume that each fiber link is bidirectional, supporting one wavelength. In Fig. 1, OXC #3 is further described with an auxiliary graph, and the transmitter and receiver pairs inside the IP/optical integrated node are also considered. If a node is selected as a tide-peak node, then this node cannot be bypassed in the

establishment of a lightpath, which makes full use of the transceivers inside the tide-peak node and guarantees the potential grooming opportunities for its arriving IP traffic.

For instance, we suppose the four nodes shown in Fig. 1 are all busy nodes under high traffic arrival rates. If there is a traffic request from IP/MPLS #1 to IP/MPLS #4, ordinary nodes will choose the MinTHV (minimum traffic hops on virtual topology) approach, which has been shown to perform the best when transceivers are more constrained resources [19], and set up the minimal number of lightpaths (IP/MPLS #1—OXC #1—OXC #3—OXC #4—IP/MPLS #4) to minimize the traffic hops on virtual topology to support the traffic. Thus, a one-hop lightpath is established, and IP/MPLS #3 is bypassed. So, at this time, when another traffic request from IP/MPLS #3 to IP/MPLS #4 arrives, neither grooming nor establishing a new lightpath is accepted, and this traffic request may be blocked. However, if we turn to our proposed tide-peak node-state-decision model and IP/Optical Node #3 is selected as the tide-peak node, then we will try to set up short lightpaths in tide-peak areas, and IP/Optical Node #3 cannot be bypassed. So, the original traffic #1 will be supported by two lightpaths (IP/MPLS #1—OXC #1—OXC #3—IP/MPLS #3 and IP/MPLS #3—OXC #3—OXC #4—IP/MPLS #4), and the transmitter and receiver pair inside IP/Optical Node #3 is utilized; thus, the new traffic request can be groomed into the second lightpath through the utilized transceivers inside IP/Optical Node #3. Therefore, by increasing the utilization of the transceivers inside the tide-peak nodes and avoiding having them be bypassed, we establish the lightpath as short as possible in tide-peak areas so as to reduce the network blocking probability.

III. FORMULATION FOR NODE-STATE-DECISION OPTIMIZATION

A. Trade-Off: Energy Efficiency Versus Blocking Performance

The optical bypass consumes little energy because it avoids using equipment like transceivers and IP

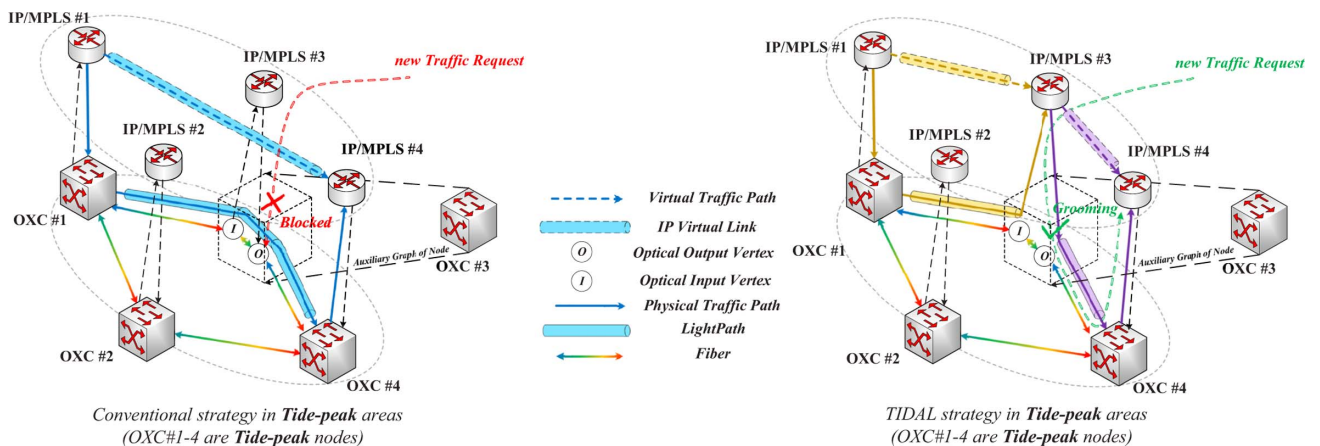


Fig. 1. Illustrative example of node-state-decision model.

router ports, which consume the majority of the used energy. Considering that the operational consumption of the other parts of the node infrastructures remains almost constant in core or metro networks, which is also irrelevant to the fluctuations of the traffic amount, here we can regard the energy consumption as proportional to the number of used transceivers [24] for simplicity.

In our node-state-decision model, if one node is selected as the tide-peak node, then this node cannot be bypassed and there will be more chances for the traffic to be groomed in the lightpath, which will enhance the network performance for traffic with a high arrival rate. However, as tide-peak nodes cannot be bypassed and the transceivers will be highly utilized, it will also result in higher energy consumption. So, there is a trade-off in the node-state-decision optimization problem: if we set all the nodes in business (high traffic) areas to be tide-peak nodes, they will achieve a better network performance with the minimum blocking probability, but the energy consumption may also increase. Our experimental simulations and analysis will later show that not every busy node needs to be selected as the tide-peak node; thus, the optimal solution to the node-state-decision optimization problem needs to be further studied.

B. MOILP Formulation

We formulate the trade-off into a MOILP to solve the problem of node-state-decision optimization considering both the energy efficiency and network performance. The notations, parameters, and variables for this model are listed below. The aim of this mathematical planning is to determine the optimal distribution of tide-peak nodes for any given traffic profile.

Given:

- $G(N, E)$: a physical topology, where N denotes the set of nodes, and E denotes the set of edges composed of fiber links.
- s, d denote the source and destination, respectively, of an end-to-end traffic request.
- i, j denote the originating and terminating nodes, respectively, of a lightpath.
- m, n denote the end points, respectively, of a physical fiber link that might occur in a lightpath.
- T : set of traffic requests.
- B : set of granularities of traffic requests.
- b_{sd}^t : granularity of traffic request t between (s, d) .
- W : numbers of wavelengths per fiber, and we assume that all the fibers carry the same number of wavelengths.
- F_{mn} : numbers of unidirectional fibers connecting from node m to node n .
- C : maximal capacity of each wavelength.
- $TR(n)$: number of transmitters inside node n .
- $RE(n)$: number of receivers inside node n .

Variables:

- π_x : integer decision variable, which takes the value zero if node x is selected as the tide-peak node.
- V_{ij} : integer variable, which denotes the number of lightpaths from node i to node j on the virtual topology.
- V_{ij}^w : integer variable, which denotes the number of lightpaths from node i to node j on wavelength w .
- $P_{mn}^{ij,w}$: binary decision variable, which takes the value one if lightpath (i, j) is routed through fiber (m, n) on wavelength w .
- R_{sd}^t : binary decision variable, which takes the value one if the traffic request t between (s, d) is successfully routed.
- $\lambda_{ij,b}^{sd,t}$: binary decision variable, which takes the value one if the traffic request t between (s, d) with granularity b employs lightpath (i, j) as an intermediate virtual link.

Optimize:

$$\text{Minimize blocking: } F_1 = \sum_{t \in T} (1 - R_{sd}^t), \quad (1)$$

$$\text{Minimize energy: } F_2 = \sum_{x \in N} \left(\sum_{j \in N} V_{xj} + \sum_{i \in N} V_{ix} \right). \quad (2)$$

Constraints:

$$\pi_x = \left(\sum_{(i,j) \in L, n \in N, w \in W} P_{xn}^{ij,w} + \sum_{(i,j) \in L, m \in N, w \in W} P_{mx}^{ij,w} \right) - \left(\sum_{j \in N} V_{xj} + \sum_{i \in N} V_{ix} \right), \quad \forall x \in N, \quad (3)$$

$$P_{mn}^{ij,w} \leq \pi_m, \quad \text{if } m \neq i, j \quad \forall w \in W, \quad (4)$$

$$P_{mn}^{ij,w} \leq \pi_n, \quad \text{if } n \neq i, j \quad \forall w \in W, \quad (5)$$

$$\sum_{j \in N} V_{ij} \leq TR(i), \quad \forall i \in N, \quad (6)$$

$$\sum_{i \in N} V_{ij} \leq RE(j), \quad \forall j \in N, \quad (7)$$

$$\sum_{w \in W} V_{ij}^w = V_{ij}, \quad \forall i, j \in N, \quad (8)$$

$$\sum_{i,j \in N} P_{mn}^{ij,w} \leq F_{mn}, \quad \forall m, n \in N \quad \forall w \in W, \quad (9)$$

$$\sum_{m \in N} P_{mi}^{ij,w} = 0, \quad \forall i, j \in N \quad \forall w \in W, \quad (10)$$

$$\sum_{n \in N} P_{jn}^{ij,w} = 0, \quad \forall i, j \in N \quad \forall w \in W, \quad (11)$$

$$\sum_{m \in N} P_{mj}^{ij,w} = V_{ij}^w, \quad \forall i, j \in N \quad \forall w \in W, \quad (12)$$

$$\sum_{n \in N} P_{in}^{ij,w} = V_{ij}^w, \quad \forall i, j \in N \quad \forall w \in W, \quad (13)$$

$$\sum_{m \in N} P_{mk}^{ij,w} = \sum_{n \in N} P_{kn}^{ij,w}, \quad \text{if } k \neq i, j \quad \forall i, j, k \in N \quad \forall w \in W, \quad (14)$$

$$\sum_{i \in N} \lambda_{id,b}^{sd,t} = R_{sd}^t, \quad \forall s, d \in N, b \in B, t \in T, \quad (15)$$

$$\sum_{j \in N} \lambda_{sj,b}^{sd,t} = R_{sd}^t, \quad \forall s, d \in N, b \in B, t \in T, \quad (16)$$

$$\sum_{i \in N} \lambda_{is,b}^{sd,t} = 0, \quad \forall s, d \in N, b \in B, t \in T, \quad (17)$$

$$\sum_{j \in N} \lambda_{dj,b}^{sd,t} = 0, \quad \forall s, d \in N, b \in B, t \in T, \quad (18)$$

$$\sum_{i \in N} \lambda_{ik,b}^{sd,t} = \sum_{j \in N} \lambda_{kj,b}^{sd,t}, \quad \text{if } k \neq s, d \quad \forall s, d, k \in N \quad \forall t \in T, \quad (19)$$

$$\sum_{t \in T} b^t \lambda_{ij,b}^{sd,t} \leq V_{ij} C, \quad \forall i, j \in N. \quad (20)$$

Optimization F_1 (1) aims to minimize the number of blockings (routing failures) in the given traffic of the network, which also means maximizing the throughput, while optimization F_2 (2) aims to minimize the number of used transceivers (and hence the used energy) of the network.

Constraint (3) ensures that the number of used transceivers should be equal to the number of lightpaths at tide-peak nodes, and if not, the node will be selected to be a tide-valley node. Constraints (4) and (5) ensure that if a node is selected as the tide-peak node, then this node should be the origin or termination of a lightpath and should not be bypassed.

Constraints (6) and (7) are about transceivers, where the number of lightpaths originating from node i should be no more than the number of transmitters at node i , while the number of lightpaths terminated at node j should be no more than the number of receivers in node j . Constraint (8) guarantees that the overall lightpaths between (i, j) should consist of all lightpaths between (i, j) on every wavelength. Constraint (9) ensures that one wavelength w on fiber (m, n) should be utilized for no more than one lightpath. Therefore, the number of lightpaths (i, j) routed through

fiber (m, n) on every possible wavelength w should be no more than the number of fibers between (m, n) .

All nodes on the physical topology should obey the basic principle of flow conservation with the wavelength-continuity constraint. Constraints (10)–(14) are *physical-layer flow conservation equations*, enforcing the proper provisioning of lightpaths over physical optical fibers. Constraint (10) ensures that the number of incoming lightpaths at node i , which is the origin of lightpath (i, j) on wavelength w , should be 0, and constraint (11) ensures that the number of outgoing lightpaths at node j , which is the termination of lightpath (i, j) on wavelength w , should be 0. Constraint (12) ensures that the number of incoming lightpaths at node j , which is the termination of lightpath (i, j) on wavelength w , should be equal to the number of lightpaths between node (i, j) on wavelength w , and constraint (13) ensures that the number of outgoing lightpaths at node i , which is the origin of lightpath (i, j) on wavelength w , should be equal to the number of lightpaths between node (i, j) on wavelength w . Constraint (14) considers the intermediate node k (k should not be i or j) of lightpath (i, j) on wavelength w , and the number of incoming lightpath flows should be equal to the number of outgoing flows at node k .

Similarly, all nodes on the virtual topology should obey the basic principle of flow conservation. Constraints (15)–(19) are *virtual-layer flow conservation equations*, ensuring that accessed traffic is routed onto relevant lightpaths. Constraint (15) ensures that for any possible i , the sum of traffic request t from node s to node d with granularity b employing lightpath (i, d) as an intermediate virtual link should be one if this traffic is successfully accessed, and constraint (16) ensures that for any possible j , the sum of traffic request t from node s to node d with granularity b employing lightpath (s, j) as an intermediate virtual link should be one if this traffic is successfully accessed. Constraint (17) ensures that for any possible i , the amount of traffic t from node s to node d with granularity b employing lightpath (i, s) as an intermediate virtual link should be zero, because s is the source of the traffic request t , and constraint (18) ensures that for any possible j , the amount of traffic t from node s to node d with granularity b employing lightpath (d, j) as an intermediate virtual link should be zero, because d is the destination of traffic request t . Constraint (19) considers the intermediate node k (k should not be i or j) of lightpath (i, j) on wavelength w , and the amount of traffic t from node s to node d with granularity b employing lightpath (i, k) as an intermediate virtual link should be equal to the amount of traffic t from node s to node d with granularity b employing lightpath (k, j) as an intermediate virtual link.

Constraint (20) ensures that the load of all traffic employing lightpath (i, j) should not exceed the overall capacity between nodes i and j .

Note that constraints (6)–(20) are general multi-hop static grooming equations, while constraints (3)–(5) are novel constraints added for the node-state-decision model.

C. Pareto Front Analysis for MOILP

Based on the above formulation, we apply the *Pareto front* principle to evaluate the trade-off between the objectives of a MOILP. Here, a Pareto front consists of points (F_1, F_2) such that the two objectives cannot be further improved at the same time. A general approach to solve the Pareto front problem is to transform the multi-objective ILP into a single-objective ILP (SOILP) by changing one of the optimization objectives into a constraint and solving it iteratively.

The MOILP is transformed into an SOILP as follows:

Given:

- β : acceptable ratio of failed routed traffic in the network.
- all parameters in the MOILP.

Optimize:

$$\text{Minimize: } F_1. \quad (21)$$

Constraints:

$$F_2 \leq f, \quad f \in \left[\left[2 \sum_{t \in T} \beta \cdot b_{sd}^t / C \right], \sum_{n \in N} (TR(n) + RE(n)) \right], \quad (22)$$

with constraints (3)–(20).

Here, f is the iterative variable. We transform F_2 into a constraint because it is relatively easier to iterate on. $\sum_{n \in N} (TR(n) + RE(n))$ is the maximum number of transceivers in the network, representing that all transceivers are used for lightpath establishment, and $\left[2 \sum_{t \in T} \beta \cdot b_{sd}^t / C \right]$ is a loose lower bound for the actual used transceivers under a given traffic load with an acceptable ratio of failed routed traffic β , and β is an alterable parameter that considers that not all traffic is successfully routed. In the iterative process, let (f_1, f_2) be a point obtained by solving the MOILP when $F_2 \leq f$, and similarly, (f'_1, f'_2) be the point when $F_2 \leq f - 1$. Then, we can acquire the Pareto front based on **Theorem 1**.

Theorem 1: If $f'_1 > f_1$ and $f'_2 < f_2$, then (f_1, f_2) is a Pareto point.

Proof: We can prove this by contradiction. If (f_1, f_2) is not a Pareto point of (F_1, F_2) , it means that F_1 and F_2 can be further optimized at the same time. Let (f''_1, f''_2) be the optimized point such that a) $f''_2 < f_2$ and $f''_1 \leq f_1$ or b) $f''_2 \leq f_2$ and $f''_1 < f_1$.

Case a): if $f''_2 < f_2$, then $f''_2 \leq f - 1$ since $f_2 < f$. When we solve, for instance, $F_2 \leq f - 1$, we should get $f'_1 \leq f''_1$. Thus, we get a contradiction: $f_1 < f'_1 \leq f''_1 \leq f_1$.

Case b): similar derivations as above.

Thus, we solve the problem of tide-peak node formulation with a feasible MOILP optimization.

IV. DYNAMIC TRAFFIC-AWARE INTELLIGENT DIFFERENTIATED ALLOCATION OF LIGHTPATH (TIDAL) SCHEME

A. Dynamic Tidal Traffic Model

In a dynamic tidal traffic scenario, the distribution of traffic requests is uneven in both the temporal and spatial domains. Generally, people are in business areas during the day, causing tide-peak nodes to operate under a huge traffic burden. Essentially, this huge traffic burden is characterized by high traffic arrival rates, as many people tend to generate a larger amount of traffic requests in a certain period of time, and the increased bandwidth demand is the aftermath of the high traffic arrival rate.

Based on the above observations, we model the dynamic tidal traffic as follows. We suppose that all the traffic has almost the same distribution of holding times. But the main difference between busy nodes and non-busy nodes is their traffic arrival rates, where the arrival rates of busy nodes are much higher than those of non-busy nodes. During the day, nodes in business areas are busy nodes with high traffic arrival rates, while the rest of the nodes (nodes in residential areas included) are non-busy nodes with low traffic arrival rates. In contrast, at night, nodes in residential areas are busy nodes, while other nodes (nodes in business areas included) are non-busy nodes.

B. Trigger for Node-State Re-decision

When the traffic is not known a priori, we need to handle the tidal traffic online with traffic requests arriving and departing successively. A node can shift between the tide-peak state and the tide-valley state with time. So, the problem is when to trigger the MOILP for node-state re-decision. We define ρ_1 as the average arrival rate of the nodes in business areas, and ρ_2 as the average arrival rate of the nodes in residential areas (where $\rho_1 \geq \rho_2$ during the daytime, and $\rho_1 \leq \rho_2$ at night). The arrival rate of those nodes in neither business areas nor residential areas is equal to the smaller one of ρ_1 and ρ_2 . We further measure the ratio between ρ_1 and ρ_2 , which is called the traffic arrival rate ratio (ARR), using

$$\text{ARR} = \rho_1 / \rho_2 \quad (23)$$

So, if $\text{ARR} = 1$, it means the traffic is uniformly distributed, and if $\text{ARR} > 1$, it means the nodes in business areas have higher traffic than nodes in residential areas. The ARR can be the decision parameter to determine the severity of the tidal traffic. Thus, we use ΔARR , which equals the current ARR minus the prior ARR, to measure the fluctuation of the tidal traffic, thereby triggering the node-state re-decision process. If the value of $|\Delta\text{ARR}|$ is larger than a decision threshold ϵ , then the MOILP program is triggered to determine the new distribution of tide-peak nodes, and only the nodes in busy areas can be selected as tide-peak nodes by the MOILP.

The input set of the MOILP is the network traffic over a reasonable amount of time (30 min or 1 h). Note that the measurements of ARR and ΔARR are periodic operations. The flowchart for node-state re-decision is shown in Fig. 2.

C. Dynamic TIDAL Algorithm

We design a dynamic TIDAL algorithm based on the decision results of the tide-peak and tide-valley nodes. Here, we apply the MOILP as the input of the dynamic algorithm. Although the traffic-grooming problem is NP-complete [19], which will cost a large amount of time to solve in a large topology, the tidal traffic also changes “slowly,” with no need for the real-time selection of tide-peak nodes. Generally, the dynamic algorithm changes its input parameters (tide-peak node distribution) every few hours, so it is feasible to apply the results of the MOILP for the dynamic situation.

In our dynamic algorithm, for every arriving traffic request, the algorithm allocates corresponding lightpaths with differentiated rules in tide-peak and tide-valley nodes, and for every departing traffic connection, the algorithm releases the resources this connection used to occupy. In the algorithm, the *currently available node* means that this node has unoccupied transceivers and its connected fiber links also have unoccupied wavelengths for new lightpaths to be established. The algorithm is shown below.

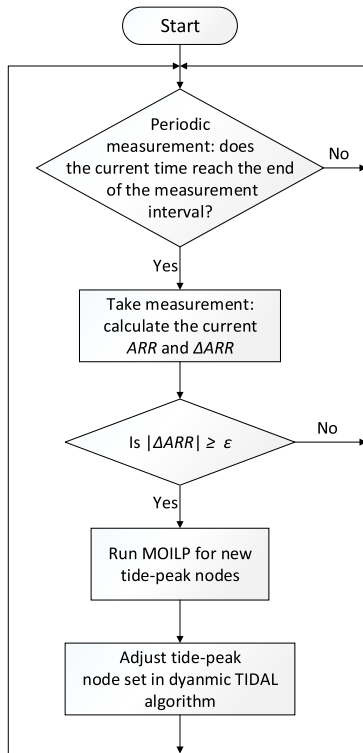


Fig. 2. Flowchart of trigger for node-state decision.

Algorithm 1 Dynamic TIDAL Algorithm

1. Initialization: $\mathcal{N}_{\text{peak}} \leftarrow$ current *tide-peak* nodes, $\mathcal{N}_{\text{valley}} \leftarrow$ current *tide-valley* nodes, ($\mathcal{N}_{\text{peak}} \cup \mathcal{N}_{\text{valley}} = \mathcal{N}$, $\mathcal{N}_{\text{peak}} \cap \mathcal{N}_{\text{valley}} = \emptyset$); $R_t \leftarrow$ arriving traffic request;
2. **if** R_t is a connection establishment request **then**
3. **if** R_t can be groomed onto IP/MPLS virtual topology via one hop **then**
4. accommodate R_t via one-hop traffic grooming;
5. **else if** R_t can be accommodated by establishing one new lightpath \mathcal{L}_t on partial topology only with nodes in current available $\mathcal{N}_{\text{valley}}$ **then**
6. establish the lightpath and then groom R_t on it;
7. **else if** R_t can be accommodated by multi-hop grooming on IP/MPLS virtual topology **then**
8. accommodate R_t via multi-hop traffic grooming;
9. **else if** R_t can be accommodated by the combination of both establishing N lightpaths \mathcal{L}_t^n and the existing IP/MPLS virtual topology **then**
10. **for** $n = 1$ to N **do**
11. **if** $\mathcal{L}_t^n \cap \mathcal{N}_{\text{peak}} = \emptyset$ **then**
12. establish lightpaths only with nodes in current available $\mathcal{N}_{\text{valley}}$ and adopt bypass if necessary;
13. **else**
14. **for** nodes $\mathcal{N}_t^{n,k} \in \mathcal{L}_t^n$, $k = 2$ to $|\mathcal{L}_t^n|$ **do**
15. **if** $\mathcal{N}_t^{n,k} \in \mathcal{N}_{\text{peak}}$ **then**
16. establish a lightpath between \mathcal{N}_t^{k-1} and \mathcal{N}_t^k ;
17. **else**
18. continue;
19. **end if**
20. **end for**
21. **end if**
22. **end for**
23. accommodate R_t on the combination of both newly established lightpaths and existing virtual links via multi-hop traffic grooming;
24. **else**
25. traffic R_t is blocked;
26. **end if**
27. **else**
28. R_t is a connection departure request, so release the resources of connection R_t ;
29. **end if**

Note that in the grooming, routing, and wavelength assignment procedure of the TIDAL algorithm, the shortest-path algorithm we adopt is the Dijkstra algorithm, and if there are multiple possibilities (several equal grooming links or available wavelengths for new lightpaths), a *First Fit* policy [25] is applied for routing and wavelength assignment.

We also analyze the time complexity of the TIDAL algorithm in a topology with K nodes. In the TIDAL algorithm, we run the Dijkstra algorithm (sentences 2–9) to get the shortest path under different conditions, and the time complexity of the Dijkstra algorithm is $O(K^2)$. A two-layer circulation (sentences 10–22, where the maximum N new lightpaths are established and each of them uses at most M tide-peak nodes, which will trigger a special lightpath establishment approach that forbids bypass in tide-peak

nodes) is applied to deal with tide-peak nodes and their related newly established lightpaths, and its complexity is $O(NM)$. As $N < K$ and $M < K$, the time complexity of the TIDAL algorithm is $O(K^2 + NM) = O(K^2)$.

V. WORKFLOW PROCEDURES

In this section, we present the actual workflow procedures of the dynamic TIDAL scheme with a software-defined architecture with the optical control agent (OCA) proposed in our previous work [26]. In this OpenFlow-enabled architecture, the OCA abstracts the optical equipment for the software-defined networking (SDN) controller and translates the OpenFlow messages for the optical equipment. The version of OpenFlow specification we adopt is 1.0.0 [27]. As shown in Fig. 3, a detailed analysis on the signaling of the entire architecture is described. It should be stated that we only analyze the signaling procedures that are relevant to the proposed TIDAL paradigm, and regular

OpenFlow signaling procedures supporting basic functions are omitted here.

A. Traffic State Acquisition and ILP Trigger

Generally, an OFPT_STATS_REQUEST message is sent to OCAs from the SDN controller to query the current state of the traffic (Step 1). Then, each OCA updates its traffic engineering database (TED) by sending the traffic statistics requests and collecting the reply messages in a specific private format corresponding to its domain (Step 2). As soon as the OCA finishes the process of the TED update, the OCA sends an OFPT_STATS_REPLY message back to the SDN controller (Step 3). The above Steps 1–3 are operated periodically, as the chart in Fig. 2 shows, and collect the information about the traffic fluctuation at certain intervals to achieve traffic awareness. Then, the controller will calculate the ARR and ΔARR based on the traffic, and decide whether to trigger the re-selection of the tide-peak

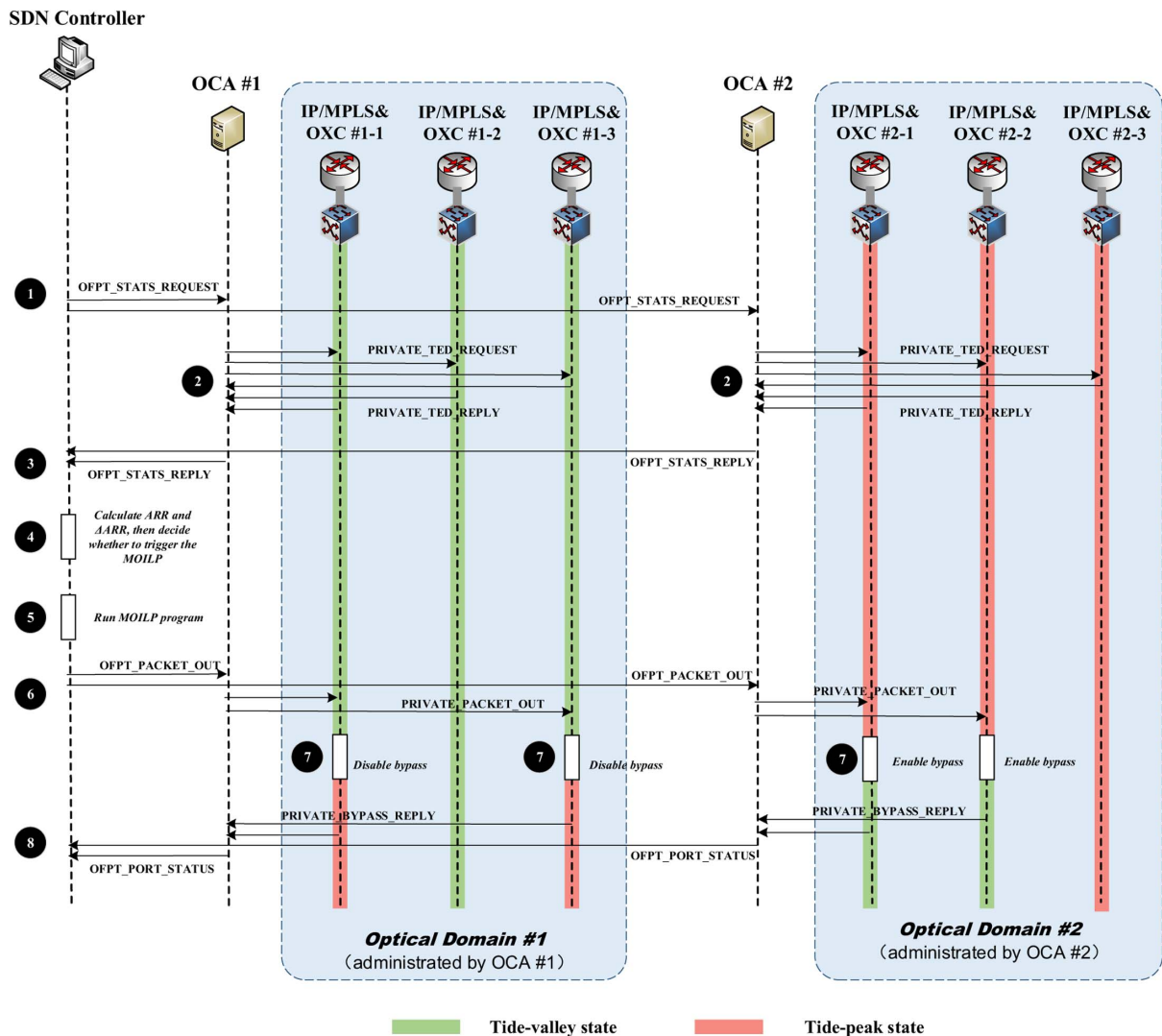


Fig. 3. Signaling from tide-peak to tide-valley with software-defined architecture [26].

nodes (Step 4). If the absolute value of ΔARR exceeds the threshold ε , the MOILP program will be executed (Step 5), or else the controller will continue to repeat Step 1 to Step 4.

B. Tide-Peak Nodes Re-configuration

After the MOILP is triggered, the SDN controller will execute the MOILP according to the current traffic situation (Step 5). The SDN controller sends the OCAs an OFPT_PACKET_OUT message, which contains the information of the tide-peak nodes re-selection results. The OCA will translate the OFPT_PACKET_OUT message into the private messages of its domain and send these messages to the relevant optical equipment (Step 6). Then, each piece of optical equipment will enable, disable, or sustain the state of bypass availability for fine-grained traffic grooming according to the instructions received (Step 7).

The optical equipment will return a reply message in the domain's private format to the corresponding OCA, and the OCA will translate and encapsulate these messages into an OFPT_PORT_STATUS message and forward it to the controller (Step 8).

VI. NUMERICAL EVALUATION

We evaluate the numerical results by our proposed MOILP and TIDAL algorithm based on stateful grooming in energy efficiency and blocking reduction perspectives. As energy efficiency is achieved by deciding the tide-peak nodes with the MOILP and configuring the nodes accordingly, it is a relatively static concept, while blocking probability is a dynamic concept. The blocking reduction is accomplished by stateful grooming with the tide-peak node constraint that bypass traffic is not allowed to route through; thus, we discuss these two problems separately.

A. Energy Efficiency Evaluation

In this section, we mainly discuss the energy efficiency achieved by the MOILP. We first use a small network (Fig. 4) for MOILP static optimization where the traffic is known a priori. The topology consists of 6 nodes and 8 links with bidirectional fibers supporting 2 wavelengths each, and all nodes are equipped with 8 tunable transceivers. There are traffic requests between any node pairs,

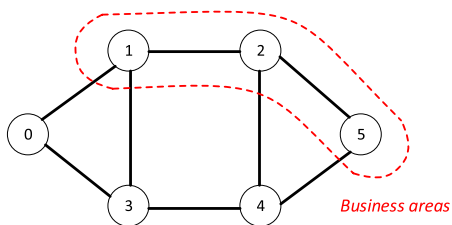


Fig. 4. Topology for static planning.

where 3 nodes in business areas have traffic 10 times (heavy tidal scenario) or 1.75 times (slight tidal scenario) higher than the other 3 nodes. The total amount of traffic requests is constant in each case, and the heavy traffic case has 1.2 times more overall traffic. As studied before, we consider that the major energy consumption is proportional to the number of used transceivers. We run the MOILP using an IBM CPLEX solver on a commercial Dell server with 2.5 GHz CPU and 32 G memory. For Fig. 5(a), the actual running time of the MOILP varies from 0.56 to 1151.72 s in different iterations, while for Fig. 5(b), this range is from 0.50 to 449.53 s.

The Pareto front of the MOILP is depicted in Fig. 5, which reveals the trade-off between energy efficiency and blocking performance intuitively. For universality and simplicity considerations, we normalize the energy consumption by the largest number of transceivers equipped in every node, which is set to be the **default point** in the graph, while the throughput is normalized by the total traffic amount. We use 1 minus throughput/total traffic to represent the ratio of blocking as the vertical axis in Fig. 5. The **grooming point** shows the largest energy consumption of conventional static multi-hop traffic grooming under tide-peak node constraints without considering energy efficiency. The **QoS strict point** is the optimal Pareto point, which values the blocking performance more than energy savings. The **QoS acceptable region** represents the points where the trade-off can gain “large” benefits with “little” compromise.

1) *Light Traffic With No Blocking in Default Points*: In the light traffic case depicted in Fig. 5(a), the baseline traffic is light and there is no blocked traffic in the default point. We investigate the network performance under the heavy tidal and slight tidal scenarios. For the heavy tidal scenario with a 10 times difference between the tide peak and tide valley, the good news that can be learned from the figure is that the energy consumption is reduced considerably (from 48% at the grooming point to 33% at the QoS strict point, represented by the black line) with no blocking performance degradation, and this point is supposed to be the optimal **QoS strict point**. The reason for this “free” energy savings lies in the fact that conventional grooming tends to provision equal lightpath capacity for all nodes according to the heaviest traffic, which performs well for uniform traffic, but causes empty or low-utilized lightpaths in tide-valley nodes in the tidal traffic scenario. So, 15% energy savings are gained from those nodes that are under a light traffic burden but dimensioned and configured as tide-peak nodes. If the tidal traffic difference become less evident (slight tidal scenario), the energy savings of the QoS strict point gained without blocking loss also becomes slight (from 46% at the grooming point to 36% at the QoS strict point, represented by the red line), which also supports the above analysis because, in this scenario, the severity of the tidal traffic is low.

Furthermore, in both scenarios, if we are not so critical about the blocking performance, we can adopt the nodes in the **QoS acceptable region**, as they stand a good balance between the energy efficiency and blocking performance,

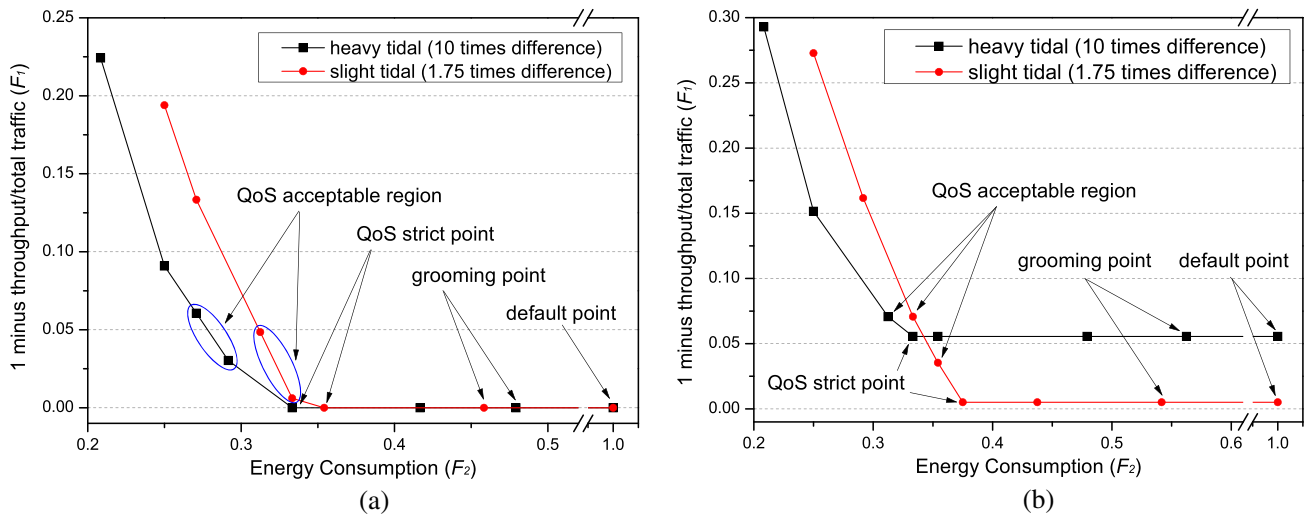


Fig. 5. Trade-off: 1 minus throughput/total traffic (F_1) versus energy consumption (F_2). (a) Limited overall traffic (all traffic routed successfully in default points). (b) 1.2 times larger overall traffic (not all traffic routed successfully in default points).

which can achieve more energy savings up to 20%–25% (from 48% at the grooming point to the QoS acceptable region in the heavy tidal scenario) or 12%–15% (from 46% at the grooming point to the QoS acceptable region in the slight tidal scenario) with a relatively acceptable blocking probability compromise of less than 3%–6% (in the heavy tidal scenario) or 1%–5% (in the slight tidal scenario). However, if we seek more energy savings beyond the region, the network QoS will deteriorate to an unacceptable level (10% or more blocking) with relatively little energy efficiency.

2) *Heavier Traffic With Acceptable Blocking in Default Points:* In Fig. 5(b), where the overall amount of traffic is 1.2 times larger than that in Fig. 5(a), we can observe that the default point no longer operates without blocking traffic, and the heavy tidal scenario has a larger blocking probability. We find that the “free” energy savings without blocking compromise can still be achieved in the QoS strict points, and the energy savings in both the heavy and light tidal scenarios become greater: the heavy scenario achieves 22% energy savings (from 56% at the grooming point to 34% at the QoS strict point, represented by the black line), while the light scenario achieves 17% (from 54% at the grooming point to 37% at the QoS strict point, represented by the red line). This is because the grooming points become larger in energy consumption due to the increase of the traffic amount. The energy consumption of the QoS strict points remains almost the same because the decisions of the node state correspond to the severity of the tidal traffic as well as the distribution of the tide-peak and tide-valley nodes, not the amount of total traffic. Another observation is that, in Fig. 5(b), the QoS acceptable region becomes smaller, and the reason is that the blocking performance increases more sharply than in the light traffic case, so given the equal acceptable blocking probability, the energy savings become less.

3) *MOILP Results for Large Topology* To verify the feasibility of the MOILP in a large topology, we further run the

MOILP in the topology in Fig. 6(a). The topology consists of 22 nodes and 38 links with bidirectional fibers supporting 2 wavelengths each, and all nodes are equipped with 10 tunable transceivers. There can be traffic requests between any node pairs, and those nodes in busy areas have ARR times more requests. We adjust the traffic ARR to evaluate the tide-peak nodes selection results of the MOILP. The tide-peak nodes are decided by the QoS strict point in each Pareto front of a different ARR, where the blocking performance is valued in preference to energy efficiency.

In Table I, we can find that as the ARR becomes larger, more nodes tend to be selected as tide-peak nodes to accommodate more traffic in busy areas. Meanwhile, we can also conclude that those nodes on the edge of a busy area are more likely to be selected as tide-peak nodes. This is because all the traffic within the busy area needs to be routed via the edge nodes to other nodes outside the busy area, and the edge nodes are then selected as tide-peak nodes that forbid bypassing to ensure the accessibility of those local requests that arrive at the edge nodes of the busy area. Meanwhile, we can also learn from the table that a fraction of the nodes in a busy area are selected as tide-peak nodes by the MOILP, which verifies the effectiveness of the MOILP on energy efficiency.

B. Blocking Reduction Evaluation

The energy efficiency evaluation solves the problem of the uneven distribution of tidal traffic in spatial domains at one moment, and now we need to consider tidal traffic with the temporal domains added, which is the dynamic case. Here, we focus on the dynamic arrivals and departures of traffic requests and the corresponding blocking performance of the TIDAL algorithm. Static analysis supports that the grooming point achieves equal throughput performance to the optimal QoS strict point; thus, in the dynamic case, the blocking probability difference between

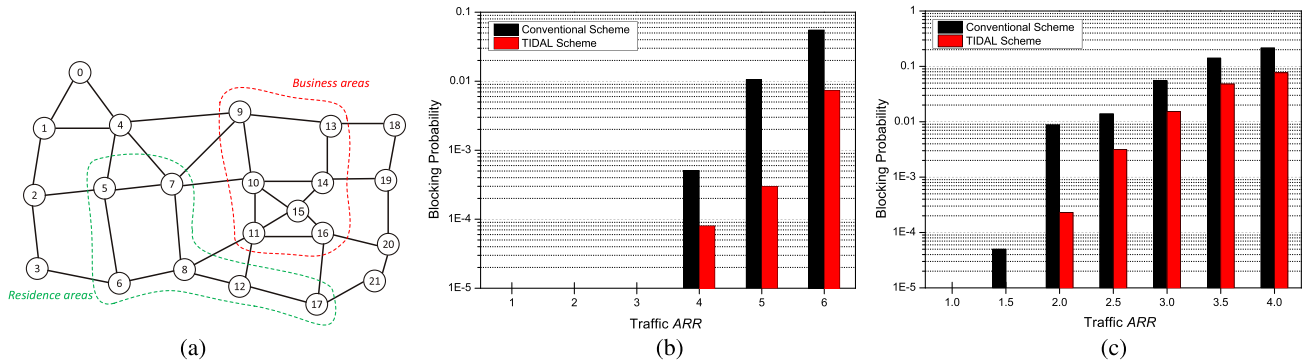


Fig. 6. Blocking probability versus traffic ARR in regional mesh networks. (a) Mesh topology for metropolitan agglomeration connections in regional network (22 nodes and 38 links). (b) Baseline traffic load = 10 Erlangs. (c) Baseline traffic load = 20 Erlangs.

TABLE I
RESULTS FOR TIDE-PEAK NODES BY THE MOILP IN
MESH TOPOLOGY FIG. 6(A)

Traffic ARR	Tide-Peak Nodes Results
2.0	16
3.0	9, 13
4.0	11, 13, 16
5.0	9, 13, 16
6.0	9, 11, 13, 16

these two points will be relatively negligible. In order to evaluate the best blocking reduction performance of the TIDAL algorithm, we apply the grooming point (all nodes in a busy area to be tide-peak nodes) of the MOILP result to be the input of the heuristic to obtain the best network performance in preference to energy efficiency.

Since tidal traffic generally takes place in large cities and metropolitan agglomerations like the San Francisco Bay Area, and the network topologies in these locations have different structures, we demonstrate our online TIDAL algorithm on two topologies that consider both regional mesh networks [Fig. 6(a)] and metro ring networks [Fig. 7(a)], where the nodes on the red dashed line are business areas that are assumed to be busy during the day, and the nodes on the green dashed line are residential areas, which are assumed to be busy during the night. The blocking performances are shown in Figs. 6 and 7, noting that the blocking probability is presented in a logarithmic scale.

1) *Regional Networks in Mesh Topology*: In the sample regional mesh network topology shown in Fig. 6(a), each fiber link is bidirectional and supports 8 wavelengths, and each node is equipped with 40 tunable transceivers. Each wavelength can support at most 100 Gbps bandwidth, and the traffic requests vary from 2.5 to 7.5 Gbps. All the traffic is characterized by Poisson arrivals ($\rho = 100,200 \text{ min}^{-1}$ as the baseline in non-busy nodes) with negative exponential holding times ($\mu = 10 \text{ min}^{-1}$).

Figure 6 shows the advantages of our proposed TIDAL scheme over the conventional scheme (MinTHV) in the aspect of blocking probability as the ARR increases.

In Fig. 6(b), the baseline node arrival rate in non-busy nodes is set to 10 Erlangs. In low ARR cases (1–3 times), as the traffic loads are smaller than the network capacity, both the conventional scheme and the TIDAL scheme perform well, with no blocked requests. However, with the increase of the ARR, the conventional scheme cannot handle the tidal traffic and the blocking probability rises sharply, while the TIDAL scheme shows a slower growth. When the ARR becomes 6 times, the conventional scheme operates with about a 6% blocking probability, while the TIDAL scheme has a less than 0.8% blocking probability, which significantly improves the network performance. This is because the TIDAL scheme can fully utilize the grooming capacity of the tide-peak nodes by avoiding being bypassed, thus accommodating more traffic when the ARR of the tidal traffic becomes larger.

Figure 6(c) shows how the network performs when the baseline node arrival rate increases. Here, we use a blocking probability of less than 20% for analytical data comparison, noting that a larger blocking probability cannot be acceptable in practice. We find that as the baseline load becomes larger, the network tends to reach the capacity with a smaller ARR, and the increase of ARR causes a larger impact on the network blocking performance. In Fig. 6(c), we observe that the TIDAL scheme can greatly reduce the blocking probability of tidal traffic by an order of magnitude, and the blocking savings become larger as the ARR becomes larger. Furthermore, we can handle 4 times ARR tidal traffic at most with an acceptable blocking probability (7%), while the conventional scheme meets obstacles (more than 20% blocking probability) in dealing with tidal traffic.

With the assistance of the static MOILP results, the dynamic TIDAL algorithm can make an accurate decision about the node state for stateful grooming, and can utilize the current network capacity to accommodate tidal traffic with a significantly lower blocking probability.

2) *Metro Networks in Interconnected-Ring Topology*: In the metro ring network shown in Fig. 7(a), there are three different kinds of nodes [28]: the two nodes illustrated as hexagons are gateways to the optical core networks, the five nodes illustrated as diamonds are hub sites to aggregate traffic, and the remaining 22 nodes are local sites.

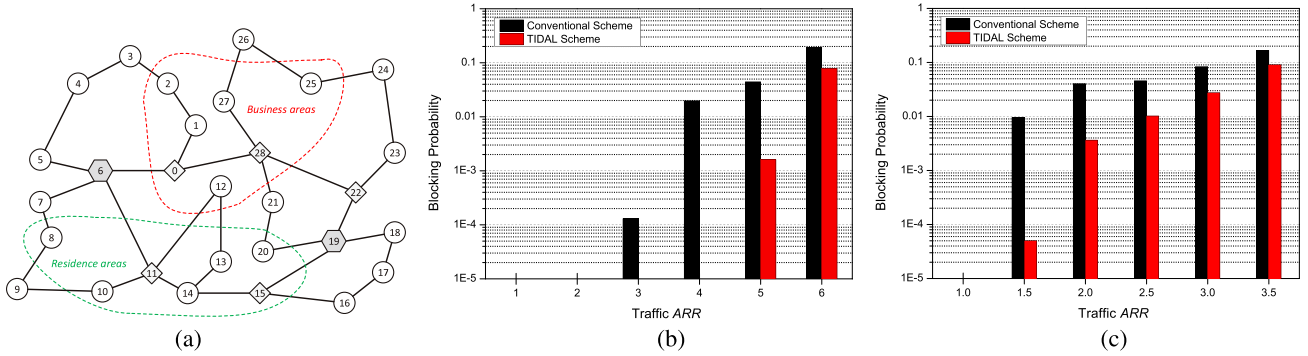


Fig. 7. Blocking probability versus traffic ARR in metro interconnected-ring networks. (a) Interconnected-ring topology for inner-city connections in metro network (29 nodes and 35 links). (b) Baseline traffic load = 5 Erlangs. (c) Baseline traffic load = 10 Erlangs.

Each fiber link is bidirectional and supports 8 wavelengths, and the nodes of the hub sites and local sites are equipped with 40 tunable transceivers. The gateway nodes are equipped with even more transceivers and fiber links, which is not shown in the graph, so as to transport the traffic to or from the optical core networks. Each wavelength can support at most 100 Gbps bandwidth, and the traffic requests vary from 2.5 to 7.5 Gbps. There are also two kinds of traffic demands, Layer 2 traffic and Internet traffic, and they are equal in traffic intensity. The Layer 2 traffic is generated between all node pairs, and the Internet traffic is generated between gateways and local or hub nodes. All the traffic is characterized by Poisson arrivals (with $\rho = 50, 100 \text{ min}^{-1}$ as the baseline in non-busy nodes) with negative exponential holding times ($\mu = 10 \text{ min}^{-1}$).

From Fig. 7, we observe that, although the topology structure and the traffic pattern are different from the previous case, our proposed TIDAL scheme can work efficiently. In Fig. 7(b), the baseline traffic load in non-busy nodes is 5 Erlangs. When the ARR is 1–2 times, both schemes have no blocking probability because the overall traffic amount is small. As the ARR increases from 3 to 4, the performance of the conventional scheme becomes worse, while the TIDAL scheme still operates with zero blocking. When the ARR is 5 or 6, the TIDAL scheme can still reduce the blocking probability by an order of magnitude. In Fig. 7(c), we see similar results to those in the regional mesh networks. When the baseline traffic becomes larger (10 Erlangs), the network may be congested in lower ARR, and as the ARR grows, the conventional scheme causes a sharp increase in the network blocking probability, while the TIDAL scheme can significantly reduce the blocking probability. We also find that the larger the ARR becomes, the larger blocking reduction is gained by the TIDAL scheme.

C. Day-Long Quasi-static Case

Based on the evaluations above, we finally present a day-long quasi-static case for tidal traffic. The typical traffic profile we used for the simulation is shown in Fig. 8(a), where the traffic load is normalized with respect to the maximum load for generality. We consider the maximum

load in both business and residential areas to be the same, because in essence, they are generated by the same amount of people at different times, and at different locations inside a city. The day-long tidal traffic in Fig. 8(a) is slotted into 12 equal periods, and in each period we use a uniform traffic load to represent the average traffic load during this 2-hour time slot. Thus, the ARR is measured every 2 hours.

From Fig. 8(a), we can observe that from 6:00 a.m. to 18:00 p.m., the business area is the busy area, while at other times, the residential area is the busy area. As there are two peaks of tidal traffic in different areas during the day, the node-state decision should be triggered at least two times when the peak shifts between business areas and residential areas. Hence, the decision threshold ϵ for the MOILP trigger here should be $\epsilon < 1.75$ in the given daily traffic profile in Fig. 8(a). The reason is that as the peak rises in business areas in the morning, the ARR increases from 1 (4:00 a.m.–6:00 a.m.) to 4 (6:00 a.m.–8:00 a.m.), and as the peak rises in residential areas in the evening, the ARR decreases from 2 (16:00 p.m.–18:00 p.m.) to 0.25 (18:00 p.m.–20:00 p.m.). Based on the results and the above observations, the goal for the Pareto front of the MOILP is to find a point where we can achieve energy savings without sacrificing blocking probability. If ϵ is larger than 1.75, the TIDAL scheme may not perform well, as the traffic peak in residential areas during the night will not be triggered. Note that ϵ should not be too small, for a smaller ϵ causes more MOILP triggers, which consume the SDN controller’s computing resources, so we determine the feasible region for ϵ , and the specific value should be decided accordingly by the specific situation in practice.

1) *Regional Networks in Mesh Topology:* In this scenario, based on the results in the dynamic case as well as the observation that the largest difference between the peak and valley is 18 times in 22:00 p.m.–24:00 p.m., we set the maximum traffic load in busy areas to be 70 Erlangs per node, with $\rho = 700 \text{ min}^{-1}$ and $\mu = 10 \text{ min}^{-1}$. The topology we use is shown in Fig. 6(a), and the business and residential areas are as shown in the figure. The network equipment parameters as well as the traffic pattern are the same as the mesh network scenario in Subsection VI.B.1.

Figure 8(b) shows the daily performances of the conventional scheme and our proposed TIDAL scheme.

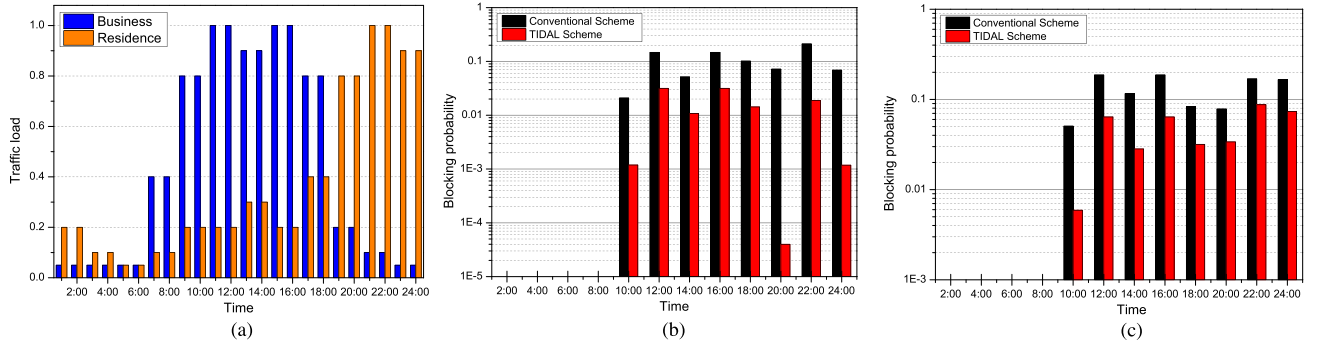


Fig. 8. Daily performance evaluation. (a) Typical day-long tidal traffic profile in business and residential areas. (b) Daily performance in regional mesh networks. (c) Daily performance in metro ring networks.

We observe that there are generally two peaks in the blocking performance: the first peak is in business areas during the daytime, and the second peak is in residential areas during the night, both of which are due to the sharp increase of the traffic volume as well as large ARRs. Our proposed TIDAL scheme can significantly reduce the blocking probability as the daily traffic varies in both the temporal and spatial domains. From 0:00 a.m. to 8:00 a.m., due to the low amount of traffic in both business and residential areas, both the conventional and our proposed TIDAL scheme perform well without any blocking. Then, from 8:00 a.m. to 18:00 p.m., the first peak of tidal traffic occurs in the business areas, and the conventional scheme meets obstacles to accommodating such a sharp increase of traffic, and its blocking probability increases up to around 15%. However, if we adopt the TIDAL scheme, the blocking probability can be reduced by an order of magnitude, with the maximum of 3% and mostly under 1%. At night, the second peak of tidal traffic arises in residential areas from 18:00 p.m. to 24:00 p.m., similar to that during the day, and the conventional scheme suffers a nearly 20% blocking probability while our proposed TIDAL scheme operates under 2%. Therefore, our proposed TIDAL scheme can reduce the impact of large ARRs of tidal traffic, and perform steadily in reducing the blocking probability, with the highest not exceeding 3%.

2) *Metro Networks in Interconnected-Ring Topology:* In this scenario, we set the maximum traffic load in busy areas to be 30 Erlangs per node, with $\rho = 300 \text{ min}^{-1}$ and $\mu = 10 \text{ min}^{-1}$, for the same reasons stated above. The topology we use is shown in Fig. 7(a), and the business and residential areas are as shown in the figure. The network equipment parameters as well as the traffic pattern are the same as the metro network scenario in Subsection VI.B.2. Figure 8(c) shows the daily performance in metro ring networks. Similar results can be drawn from the figure: namely, in low load periods (0:00 a.m.–8:00 a.m.), both schemes achieve no blocking, and as the peak rises in business areas around noon, the TIDAL scheme achieves a significant blocking reduction compared to the conventional scheme. At night, it also works well as the peak traffic shifts to residential areas. Hence, we conclude that the TIDAL scheme acts effectively in both regional mesh networks as well as metro ring networks.

VII. CONCLUSION

In this paper, we presented a comprehensive study on applying stateful grooming to achieve an energy-efficient performance enhancement in IP-over-optical networks to tackle the tidal traffic problem. Stateful grooming was first proposed to accommodate the temporal and spatial variability of tidal traffic according to the network state. We exploited the Pareto front principle to analyze the trade-off between energy efficiency and blocking performance in the problem of node-state-decision optimization. We then proposed an online scheme to handle the dynamic tidal traffic effectively with energy-efficient node-state-decision results. The illustrative numerical results show that we can achieve considerable energy savings by deciding on the tide-peak node selection through the MOILP instead of setting all the nodes in busy areas to be tide-peak nodes in the static case. Under dynamic scenarios, our proposed online TIDAL scheme can intelligently adjust the decision of tide-peak nodes as well as reduce the network blocking probability significantly. We also simulated a day-long tidal traffic scenario to demonstrate the performance of the proposed scheme. All these dynamic demonstrations were based on both mesh networks and ring networks, considering the regional megalopolis scenario (tidal traffic in several adjacent cities) and the metro scenario (tidal traffic inside one city). Above all, our work solves the tidal traffic problem and achieves a better service performance with energy-efficiency considerations.

ACKNOWLEDGMENT

This work was supported in part by the National 973 Program (Grant No. 2014CB340104/05), the National Natural Science Foundation of China (NSFC) (Grant Nos. 61201188 and 61321004), the Tsinghua Fudaoyuan Research Fund, and Networks Lab at UC Davis. Parts of this work were presented at the OptoElectronics and Communications Conference (OECC), Shanghai, China, July 2015.

REFERENCES

- [1] A. Martinez, M. Yannuzzi, V. Lopez, D. Lopez, W. Ramirez, R. Serral-Gracia, X. Masip-Bruin, M. Maciejewski, and J. Altmann, "Network management challenges and trends

- in multi-layer and multi-vendor settings for carrier-grade networks," *IEEE Commun. Surv. Tutorials*, vol. 16, no. 4, pp. 2207–2230, 2014.
- [2] X. H. Yuan, X. Ji, H. Chen, B. Chen, and G. Q. Chen, "Urban dynamics and multiple-objective programming: A case study of Beijing," *Commun. Nonlinear Sci. Numer. Simul.*, vol. 13, no. 9, pp. 1998–2017, Nov. 2008.
- [3] Cisco, "The zettabyte era: Trends and analysis," Cisco Visual Networking Index White Paper, May 2015 [Online]. Available: http://www.cisco.com/c/en/us/solutions/collateral/service-provider/visual-networking-index-vni/VNI_Hyperconnectivity_WP.pdf.
- [4] Cisco, "Cisco visual networking index: Global mobile data traffic forecast update, 2015–2020," Cisco Visual Networking Index White Paper, Feb. 2015 [Online]. Available: http://www.cisco.com/c/en/us/solutions/collateral/service-provider/visual-networking-index-vni/white_paper_c11-520862.pdf.
- [5] Y. Zhang, P. Chowdhury, M. Tornatore, and B. Mukherjee, "Energy efficiency in telecom optical networks," *IEEE Commun. Surv. Tutorials*, vol. 12, no. 4, pp. 441–458, 2010.
- [6] Z. Niu, "TANGO: Traffic-aware network planning and green operation," *IEEE Wireless Commun.*, vol. 18, no. 5, pp. 25–29, Oct. 2011.
- [7] M. Ahmed, I. Ahmad, and D. Habibi, "Green wireless-optical broadband access network: Energy and quality-of-service considerations," *J. Opt. Commun. Netw.*, vol. 7, no. 7, pp. 669–680, July 2015.
- [8] R. Wang, H. H. Lee, S. S. Lee, and B. Mukherjee, "Energy saving via dynamic wavelength sharing in TWDM-PON," *IEEE J. Sel. Areas Commun.*, vol. 32, no. 8, pp. 1566–1574, Aug. 2014.
- [9] A. Ahmad, A. Bianco, E. Bonetto, L. Chiaraviglio, and F. Idzikowski, "Energy-aware design of multilayer core networks [Invited]," *J. Opt. Commun. Netw.*, vol. 5, no. 10, pp. A127–A143, Oct. 2013.
- [10] E. Bonetto, L. Chiaraviglio, F. Idzikowski, and E. Le Rouzic, "Algorithms for the multi-period power-aware logical topology design with reconfiguration costs," *J. Opt. Commun. Netw.*, vol. 5, no. 5, pp. 394–410, May 2013.
- [11] A. Morea, O. Rival, N. Brochier, and E. Le Rouzic, "Datarate adaptation for night-time energy savings in core networks," *J. Lightwave Technol.*, vol. 31, no. 5, pp. 779–785, Mar. 2013.
- [12] G. Rizzelli, A. Morea, M. Tornatore, and O. Rival, "Energy efficient traffic-aware design of on-off multi-layer translucent optical networks," *Comput. Netw.*, vol. 56, no. 10, pp. 2443–2455, 2012.
- [13] A. Coiro, M. Listanti, A. Valenti, and F. Matera, "Reducing power consumption in wavelength routed networks by selective switch off of optical links," *IEEE J. Sel. Top. Quantum Electron.*, vol. 17, no. 2, pp. 428–436, 2011.
- [14] Y. Zhang, M. Tornatore, P. Chowdhury, and B. Mukherjee, "Energy optimization in IP-over-WDM networks," *Opt. Switching Netw.*, vol. 8, no. 3, pp. 171–180, 2011.
- [15] C. Lange and A. Gladisch, "Energy efficiency limits of load adaptive networks," in *Optical Fiber Communication Conf. (OFC)*, San Diego, 2010, paper OWY2.
- [16] Z. Zhong, N. Hua, H. Liu, Y. Li, and X. Zheng, "Considerations of effective tidal traffic dispatching in software-defined metro IP over optical networks," in *Proc. OptoElectronics and Communications Conf. (OECC)*, Shanghai, China, 2015.
- [17] K. Zhu and B. Mukherjee, "Traffic grooming in an optical WDM mesh network," *IEEE J. Sel. Areas Commun.*, vol. 20, no. 1, pp. 122–133, Jan. 2002.
- [18] H. Zhu, H. Zang, K. Zhu, and B. Mukherjee, "A novel generic graph model for traffic grooming in heterogeneous WDM mesh networks," *IEEE/ACM Trans. Netw.*, vol. 11, no. 2, pp. 285–299, Apr. 2003.
- [19] B. Mukherjee, *Optical WDM Networks*. Springer, 2006, pp. 621–683.
- [20] K. Zhu and B. Mukherjee, "A review of traffic grooming in WDM optical networks: Architectures and challenges," *Opt. Netw. Mag.*, vol. 4, no. 2, pp. 55–64, 2003.
- [21] X. Wan, Y. Li, H. Zhang, and X. Zheng, "Dynamic traffic grooming in flexible multi-layer IP/optical networks," *IEEE Commun. Lett.*, vol. 16, no. 12, pp. 2079–2082, Dec. 2012.
- [22] S. De Maesschalck, M. Pickavet, D. Colle, and P. Demeester, "Multi-layer traffic grooming in networks with an IP/MPLS layer on top of a meshed optical layer," in *Proc. IEEE GLOBECOM*, 2003, pp. 2750–2754.
- [23] S. De Maesschalck, M. Pickavet, D. Colle, Q. Yan, S. Verbrugge, B. Puype, and P. Demeester, "Efficient multi-layer traffic grooming in an IP/MPLS-over-optical network," *Eur. Trans. Telecommun.*, vol. 16, pp. 329–347, 2005.
- [24] G. Shen and R. S. Tucker, "Energy-minimized design for IP over WDM networks," *J. Opt. Commun. Netw.*, vol. 1, no. 1, pp. 176–186, June 2009.
- [25] H. Zang, J. P. Jue, and B. Mukherjee, "A review of routing and wavelength assignment approaches for wavelength-routed optical WDM networks," *Opt. Netw. Mag.*, vol. 1, no. 1, pp. 47–60, Jan. 2000.
- [26] Z. Zhong, X. Chen, N. Hua, Y. Li, and X. Zheng, "Unified control for IP over optical transport networks based on software-defined architecture," in *Proc. Asia Communications and Photonics Conf. (ACP)*, Shanghai, China, 2014.
- [27] Open Networking Foundation, "OpenFlow Specification 1.0.0," Dec. 2009 [Online]. Available: <https://www.opennetworking.org/images/stories/downloads/sdn-resources/onf-specifications/openflow/openflow-spec-v1.0.0.pdf>.
- [28] S. Ishida and I. Nishioka, "Software-defined packet optical transport networks offering multiple services," in *Optical Fiber Communication Conf. (OFC)*, Anaheim, 2013, paper NTu3F.1.

Zhizhen Zhong (S'15) received a B.E. from Tsinghua University, Beijing, China, in 2014, and is now working toward a Ph.D. at Tsinghua University. He is also a visiting Ph.D. student at the University of California, Davis, under the supervision of Prof. Biswanath Mukherjee. His research interests include software-defined optical networks, traffic grooming, and energy efficiency in optical networks. He is a student member of the IEEE and OSA.

Nan Hua (M'07) received his B.S. and Ph.D. degrees in electronic engineering from Tsinghua University, Beijing, China, in 2003 and 2009, respectively. He is now an assistant professor with the Department of Electronic Engineering at Tsinghua University. Dr. Hua has authored or coauthored more than 70 publications and is the holder of more than 10 issued patents. His current research interests include the control and management of optical networks, all-optical switching technologies, and enabling technologies for multi-domain heterogeneous networks. Dr. Hua is a member of the IEEE Photonics Society, the IEEE Communications Society, and The Optical Society (OSA).

Massimo Tornatore (S'03-M'07-SM'13) received a M.Sc. (Laurea) in telecommunications engineering and a Ph.D. in information engineering from the Politecnico di Milano, Milan, Italy, in

2001 and 2006, respectively. He is currently an associate professor with the Department of Electronics, Information and Bioengineering at Politecnico di Milan, and an adjunct associate professor in the Computer Science Department at the University of California, Davis, USA. He is the coauthor of about 190 conference and journal papers. His research interests include design, energy efficiency, traffic grooming in optical networks, and group communication security. Dr. Tornatore is a co-winner of six best paper awards from IEEE-sponsored conferences.

Yao Li received her B.S. from Tsinghua University in Beijing, China, in 2010, and is now a Ph.D. candidate in the Department of Electronic Engineering at Tsinghua University. Her research interests include spatial division multiplexing in optical networks and datacenter networks.

Haijiao Liu received a B.S. from Tsinghua University, Beijing, China, in 2011, and is now a Ph.D. candidate in the Department of Electronic Engineering at Tsinghua University, Beijing, China. His research interests include networking, control, and management of intelligent optical communication networks.

Chen Ma received a B.S. in communication engineering in 2009 and an M.S. in signal and information processing in 2012 from North China Electric Power University. He was also a visiting student at the University of California, Davis, USA, from September 2014 to September 2015. He is now working toward a Ph.D. degree at Beijing University of Posts and Telecommunications in communication and information systems. His research interests include the survivability and virtualization of optical networks.

Yanhe Li (M'99) received a B.S. and an M.S. from the Department of Electronic Engineering, Tsinghua University, Beijing, China, in 1983 and 1987, respectively. Since 1983, he has been working within the Department of Electronic Engineering at Tsinghua University, where he is now a full professor. He has published more than 100 papers. His current research is focused on software-defined optical networks, optical networks, and microwave photonics. Prof. Li is a fellow of the Electronics Society of China, a senior member of the Optical Society of China, and a member of The Optical Society (OSA).

Xiaoping Zheng received his B.S. from Zhongshan University in 1986, his M.S. from Southeast University in 1994, and his Ph.D.

from Tsinghua University in 1998. Since 1998, he has been working within the Department of Electronic Engineering at Tsinghua University, where he is now a full professor. He was awarded 4 prizes by the Chinese Governmental Ministries for his scientific contributions and invention achievements, and has authored and coauthored more than 200 papers. He holds 20 patents. His research activities are mainly focused on heterogeneous optical networks, software-defined optical networks, and microwave photonics. Prof. Zheng was the member of the Expert Group that was responsible for drafting the strategic program of the High Performance WideBand Communication Network during the tenth five-year plan of China. He is the standing director of the Beijing Society of Optics.

Biswanath Mukherjee (S'82-M'87-F'07) received a B.Tech. (Hons.) from the Indian Institute of Technology, Kharagpur, India, in 1980, and a Ph.D. from the University of Washington, Seattle, USA, in 1987. He is a Distinguished Professor at the University of California, Davis, where he has been working since 1987; he served as the chair of the Department of Computer Science from 1997 to 2000. He served a five-year term as a founding member of the Board of Directors of IPLocks, Inc., a Silicon Valley startup company (acquired by Fortinet). He has served on the technical advisory boards of a number of startup companies, most recently Teknovus (acquired by Broadcom), Intelligent Fiber Optic Systems, and LookAhead Decisions Inc. He is author of the textbook *Optical WDM Networks* (New York: Springer, 2006), and editor of *Springer's Optical Networks Book Series*. Dr. Mukherjee co-received the Optical Networking Symposium Best Paper Award at the IEEE Globecom 2007 and 2008 conferences. He co-received the 1991 National Computer Security Conference Best Paper Award. He received the 2004 UC Davis Distinguished Graduate Mentoring Award. He serves or has served on the editorial boards of eight journals, most notably *IEEE/ACM Transactions on Networking* and *IEEE Network*. In addition, he has guest edited Special Issues of *Proceedings of the IEEE*, the *IEEE/OSA Journal of Lightwave Technology*, the *IEEE Journal on Selected Areas in Communications*, and *IEEE Communications*. He served as the Technical Program Chair of the IEEE INFOCOM '96 conference. He served as the Technical Program Co-Chair of the IEEE/OSA Optical Fiber Communication Conference (OFC) 2009, and the General Co-Chair of OFC 2011. He was the Steering Committee Chair of the IEEE Advanced Networks and Telecom Systems (ANTS) Conference, and was the General Co-Chair of ANTS in 2007 and 2008. He is an IEEE Fellow.